

# A Newly Developed Non-Cyanide Electroless Gold Plating Method Using Thiomalic Acid as a Complexing Agent and 2-Aminoethanethiol as a Reducing Agent

Jae-Ho Han<sup>1,†</sup>, Jae-Bong Lee<sup>2,†</sup>, Nguyen Van Phuong<sup>3</sup>, and Dong-Hyun Kim<sup>3</sup>

<sup>1</sup>ECtech Co.,Ltd 301,14, Garam-ro, Seo-gu, Incheon City, Republic of Korea

<sup>2</sup>School of Advanced Materials Engineering, Kookmin University, 77 Jeongneung-ro, Seongbuk-gu, Seoul 02707, Republic of Korea

<sup>3</sup>MSC Co., Ltd. 75, Namdongseo-ro (118B-15L), Namdong-gu, Incheon City 21698, Republic of Korea

(Received March 18, 2022; Revised April 25, 2022; Accepted April 25, 2022)

A versatile method for performing non-cyanide electroless gold plating using thiomalic acid (TMA) as a complexing agent and 2-aminoethanethiol (AET) as a reducing agent was investigated. It was found that TMA was an excellent complexing agent for gold. It can be used in electroless gold plating baths at a neutral pH with a high solution stability, makes it a potential candidate to replace conventional toxic cyanide complex. It was found that one gold atomic ion could bind to two TMA molecules to form the [2TMA-Au<sup>+</sup>] complex in a solution. AET can be used as a reducing agent in electroless gold plating solutions. The highest current density was obtained at electrode rotation rate of 250 to 500 rpm based on anodic and cathodic polarization curves with the mixed potential theory. Increasing AET concentration, pH, and temperature significantly increased the anodic polarization current density and shifted the plating potential toward a more negative value. The optimal gold ion concentration to obtain the highest current density was 0.01 M. The cathodic current was higher at a lower pH and a higher temperature. The current density was inversely proportional to TMA concentration.

**Keywords:** Electroless gold, Non-cyanide gold, Thiomalic acid, 2-Aminoethanethiol

## 1. Introduction

Gold is widely used for surface finishing in the electronics industry because of its many advantages, such as high electrical conductivity, excellent solderability, high reliability, and high corrosion resistance [1-4]. Gold is typically plated onto electronic components and printed circuit boards through two main processes: immersion plating such as electroless nickel-immersion gold (ENIG), and electroless gold plating [3-7].

Traditional gold plating baths using potassium gold cyanide,  $\text{KAu}(\text{CN})_2$  as the source of gold, have served well for many years for various applications in the electronics industry because of their excellent stability and coating performance [8-12]. However, cyanide is a highly toxic chemical, and cyanide-containing plating solutions are generally operated in the alkaline range,

which can erode the photoresists and other materials used in the packaging of high-density circuits. Thus, use of a non-cyanide gold plating system has become a developmental trend in industrial production [1,3,4]. Several non-cyanide gold plating baths have been developed, and most of them use gold salts, such as  $\text{NaAuCl}_4$ ,  $\text{Na}_3\text{Au}(\text{SO}_3)_2$ ,  $\text{Na}_3\text{Au}(\text{S}_2\text{O}_3)_2$ , or some mixture of them [11,13-19]. These gold plating baths are not highly stable; moreover, they usually operate at alkaline pH. Therefore, their applications are generally quite limited.

In electroless gold plating solutions, some conventional reducing agents (such as hypophosphite, formaldehyde, hydrazine, borohydride, L-cysteine, thiourea, and dimethylamine borane) have been investigated, while borohydride and dimethylamine borane are the ones most commonly used [19-23]. These baths operate in a strongly alkaline medium and use potassium gold cyanide as the gold source. A number of different reducing agents (such as L-cysteine [16], 2-mercaptosuccinic acid [17], thiourea,

<sup>†</sup>Corresponding author: hanege@nate.com, leejb@kookmin.ac.kr  
J.H. Han: C.E.O, J.-B. Lee: Professor, N.V. Phuong: Researcher, D.H. Kim: C.E.O.

N-methylthiourea, 1-acetyl-2-thiourea [15], and ascorbic acid [24,25]) have been reported in other work. However, in general, the limitations of the electroless gold process include: a generally low plating rate, complex chemistry of the baths, sensitivity to organic and inorganic contamination, and very short lifetime of a bath.

It should be noted that two critical components of an electroless gold plating bath are a complex ligand to bond with gold ions, and the reducing agent [10,12,26]. In this work, thiomalic acid (TMA) or mercaptosuccinic acid was used as a complexing agent for gold ions. Actually, several gold thiol complexes have been used as drugs to treat rheumatoid arthritis for more than half a century [27,28]. Gold ions can bond with sulfur atoms in thiol compounds to form a complex with greater stability than the solution containing gold ions only. TMA is a dicarboxylic acid containing a thiol functional group and is presented as R-SH, where an S atom can bond with  $\text{Au}^+$  to form a [R-S-Au] complex. Takeuchi *et al.* [16]. reported that TMA can be used as a complexing agent for gold ions in an electroless gold plating bath. They reported that gold ions could bond with TMA to form a TMA- $\text{Au}^+$  complex in a solution used for an electroless plating process at neutral pH using L-cysteine as reducing agent. Table 1 shows the standard electrode potentials ( $E^0$ ) of gold ions with different complexing agents [20,29]. Lower reduction potential indicates that the complex has higher stability. As can be seen, the complexing agent that forms the most stable complex with gold ions is a cyanide compound with  $E^0 = -0.65$  V vs. SHE (Standard Hydrogen Electrode). The thio compounds (R-SH) also exhibit low reduction potentials and are expected to replace the cyanide compound for complexing with gold ions. Among non-cyanide complexes, the thio compounds showed more negative reduction potential than did thiourea,  $\text{S}_2\text{O}_3^{2-}$ ,  $\text{SO}_3^{2-}$ ,  $\text{OH}^-$ ,  $\text{NH}_4^+$ , or  $\text{SCN}^-$ . AET (2-aminoethanethiol or cysteamine ( $\text{HSCH}_2\text{CH}_2\text{NH}_2$ )) is a stable aminothiols containing both amine and thiol functional groups.

Takeuchi *et al.* theoretically predicted the reducing ability of compounds by molecular orbital method to select a new type of reducing agent for the cyanide-free electroless Au plating solution [16,30]. In this report, the lowest unoccupied molecular orbital (LUMO) and highest occupied molecular orbital (HOMO) were calculated for several thio-compounds using CS (Cambridge Soft) Mopac.

**Table 1. Standard electrode potentials ( $E^0$ ) of gold ions with different complexing agents**

Ligand	Complex	$E^0$ (V vs. SHE)
$\text{H}_2\text{O}$	$\text{Au}(\text{H}_2\text{O})_2^+$	1.68
	$\text{Au}(\text{H}_2\text{O})_4^{3+}$	1.50
$\text{Cl}^-$	$\text{AuCl}_2^-$	1.15
	$\text{AuCl}_4^-$	0.92
$\text{SCN}^-$	$\text{Au}(\text{SCN})_2^-$	0.67
	$\text{Au}(\text{SCN})_4^-$	0.64
$\text{I}^-$	$\text{AuI}_2^-$	0.58
	$\text{AuI}_4^-$	0.57
$\text{NH}_3$	$\text{Au}(\text{NH}_3)_4^{3+}$	0.56
$\text{OH}^-$	$\text{Au}(\text{OH})_4^-$	0.48
Thiourea	$\text{Au}(\text{Thio})_2^+$	0.38
$\text{S}_2\text{O}_3^{2-}$	$\text{Au}(\text{S}_2\text{O}_3)_2^{3-}$	0.15
$\text{SO}_3^{2-}$	$\text{Au}(\text{SO}_3)_2^{3-}$	0.06
R-SH	$\text{Au}(\text{R-S})^{2-}$	-0.5 ~ -0.6
$\text{CN}^-$	$\text{Au}(\text{CN})_2^-$	-0.65

As a result, it has been announced that among several thio-compounds, aminoethanethiol can be used as a reducing agent for electroless plating. The difference in energy between these two frontier orbitals can be used to predict the strength and stability of transition metal complexes. And it is explained that the energy gap of LUMO-HOMO is a factor that determines the reduction rate of electroless plating.

AET can be self-oxidized to supply electrons for autocatalytic plating reactions; however, the use of AET as a reducing agent was not found in any report. Only a single ancient Japanese article reported that AET could be used as a reducing agent in electroless silver plating [31]. Thus, it is expected that AET could also be used as a reducing agent for electroless gold plating baths.

Therefore, in this study, AET was used as the reducing agent and TMA was used as the complexing agent for the electroless gold plating process. The effects of the electrode rotation rate, AET concentration,  $\text{Au}^+$  concentration, TMA concentration, temperature, and pH were systematically investigated by measuring anodic/cathodic polarization curves, and using the mixed potential theory to interpret the electroless plating process that occurred.

## 2. Experimental

### 2.1. Preparation of a TMA-gold solution

A portion (10.00 g) of gold chloride trihydrate ( $\text{HAuCl}_4 \cdot 3\text{H}_2\text{O}$ , 99% purity, Kojima Chemicals Co.) was dissolved in 20 mL of deionized water ( $18.2 \text{ M}\Omega \cdot \text{cm}^{-1}$ ) while stirring. After it was completely dissolved, 30 mL of  $\text{NH}_3$  (29%) was added into the dissolved gold solution to precipitate of  $\text{Au}_2\text{O}_3 \cdot 2\text{NH}_3$  or  $\text{Au}_2\text{O}_3 \cdot 3\text{NH}_3$ . After precipitation was complete, the precipitate was separated from the solution using Advantec 5C (1  $\mu\text{m}$ , thickness 0.22 mm) filter paper. The precipitate was washed with deionized water until the odor of ammonia was removed. The precipitate was then transferred to a 250 mL flask. Next, 100 mL of water and 12.25 g of TMA were added. The precipitate dissolved slowly, while stirring was continued for 5 h. The solution was then adjusted to pH 7.0 using a 4.0 M KOH solution, followed by filtration using 5C filter paper. Finally, the filtered solution was adjusted with deionized water to 250 mL to have a final solution containing 0.08 M TMA and 0.10 M gold ions (19.7 g/L). This was called the TMA-Au solution. The gold concentration was confirmed using atomic absorption spectroscopy (AAS).

### 2.2. Capillary electrophoresis experiment

The capillary electrophoresis (CE) experiment was performed using an Agilent HP3D capillary electrophoresis system (Agilent Technologies). The buffer solution contained 10 mM imidazole, 5 mM 2-hydroxy-iso-butyric acid, 2 mM 18-crown-6, and 2 mM acetic acid. The capillary electrophoresis system comprised a 15 kV constant voltage supply with an uncoated fused-silica capillary length of 600 mm, and operated at 20 °C.

### 2.3. Anodic and cathodic polarization curves

Electrochemical measurements were performed using an ECI QualiLab Cyclic Voltammetric Stripping (CVS) plating bath analyzer (QL-10EZ, ECI Technology) connected to a three-electrode electrochemical cell. A 10  $\text{mm}^2$  platinum rotating disc electrode (RDE), a stainless-steel rod, and a saturated calomel electrode (SCE) were used as the working, counter, and reference electrode, respectively. The linear sweep voltammetry was scanned from 0.2 to  $-0.6 \text{ V}$  with a scan rate of 10 mV/s at various rotation rates from 0 to 2000 rpm.

### 2.4. Electroless gold plating solution

Table 2 shows the chemical composition, test condition, and the basic electroless gold solution. All chemicals were purchased from the Tokyo Chemical Industry. The effects of each factor, such as the electrode rotation rate, AET concentration,  $\text{Au}^+$  concentration, TMA concentration, temperature, and pH, were systematically investigated.

## 3. Results and discussion

### 3.1. Formation of a TMA-gold complex

First, the existence of the Au-TMA complex and the coherence ratio between them in the solution were studied using CE. In this CE set of conditions, the migration time of  $\text{Au}^+$ , TMA-Au, and TMA were 4.57, 4.67, and 6.57 min, respectively. Fig. 1a shows the CE calibration

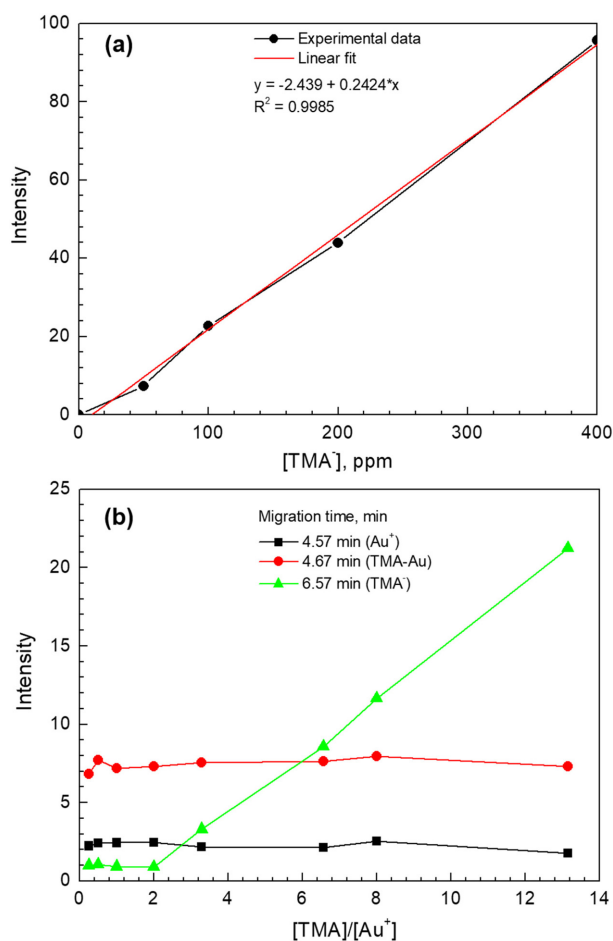


Fig. 1. CE calibration curve of the basic TMA solution (a) and CE peak intensities of  $\text{Au}^+$ , TMA-Au, and TMA at different [TMA]/[Au<sup>+</sup>] concentration ratios. The migration time of  $\text{Au}^+$ , TMA-Au, and TMA was 4.57, 4.67, and 6.57 min, respectively

curve of the basic TMA solution with a concentration range from 0 to 400 ppm. It was confirmed that the peak intensity of the migration time at 6.57 min linearly increased with increasing TMA concentration. This result indicated that the TMA concentration in the solution could be quantitatively analyzed using CE. Fig. 1b presents the CE peak intensities of  $\text{Au}^+$ , TMA- $\text{Au}^+$ , and TMA of solutions containing 0.01 M  $\text{Au}^+$ , with molar ratios of  $[\text{TMA}]/[\text{Au}^+]$  from 0.25 to 13.2. The result shows that the peak intensities of  $\text{Au}^+$  and TMA- $\text{Au}^+$  are constant with different  $[\text{TMA}]/[\text{Au}^+]$  concentration ratios, but the peak intensity of TMA linearly increases with increase in the  $[\text{TMA}]/[\text{Au}^+]$  ratio when this ratio is  $> 2$ . This means that when the ratio  $[\text{TMA}]/[\text{Au}^+] < 2$ , TMA is used to form the complex with  $\text{Au}^+$ . Free TMA only increases when this ratio is  $> 2$ . This result indicates that TMA can act as a complexing agent with gold ions to form TMA- $\text{Au}^+$  with a molar ratio of 2:1. This result is also consistent with another study in the field of pharmaceuticals where they concluded that gold ions and TMA could form complexing compounds with the same molar ratio of TMA and  $\text{Au}^+$ [28].

### 3.2. Anodic and cathodic polarization of electroless gold solution

The electroless metal plating processes have been identified as mixed potential systems. It has been suggested that the electroless plating mechanisms can be predicted from the polarization curves for the anodic and cathodic partial currents [16,20,32]. Fig. 2 shows the anodic and cathodic polarization curves of an electroless gold plating solution using TMA as a complexing agent and AET as a reducing agent, performed in the basic solution as Table 2. The anodic curve was measured in the solution with the absence of  $\text{Au}^+$  ions, while the cathodic curve was measured in the absence of AET. The plating rate of the electroless plating process can be calculated by the plating current density ( $i$ ) at the mixed potential through the partial anodic current ( $i_a$ ) or the partial cathodic current ( $i_c$ ). When the reaction is at equilibrium, the net current is zero ( $i_a + i_c = 0$ ) and the electroless plating current is determined by  $i = i_a = -i_c$ . The potential at equilibrium is designated as the mixed potential of the electroless plating process [16,20,33]. In the polarization curves, the interpreted current density (i.e.,

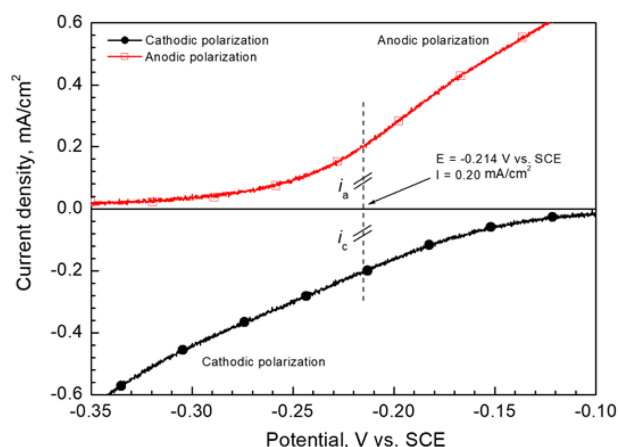


Fig. 2. Anodic and cathodic polarization curves of the basic electroless gold plating solution (Table 2)

Table 2. Composition of the basic electroless gold plating solution and test condition

Parameter	Test condition	Base
$\text{KH}_2\text{PO}_4$	0.075 M	0.075 M
TMA-Au	0.005~0.1 M	0.01 M
TMA	0.08~0.40 M	0.24 M
AET	0.05~1.2 M	0.40 M
Temp.	20~80 °C	80 °C
pH	4.0~10.0	7.0
Rotation rate	0~2000 rpm	500 rpm

plating current density) was 0.20  $\text{mA}/\text{cm}^2$ , and potential was  $-0.214$  V vs. SCE. This result suggests that the process of electroless gold plating can occur in gold solution using TMA as a complexing agent and AET as a reducing agent at pH 7.0.

### 3.3. Effect of several factors on the electroless gold plating bath

Fig. 3a displays the anodic and cathodic polarization curves of the basic electroless gold solution at different electrode rotation rates from 0 to 2000 rpm. The anodic current density increases with increase in the electrode rotation rate, especially from 0 to 500 rpm. For the cathodic polarization curves, the highest cathodic current density is obtained at the electrode rotation rate of 500 rpm. Using the mixed potential theory, the plating current density at the mixed potential and plating potential which is mixed potential were interpreted and from Fig. 3b. The plating current density at mixed potential rapidly

increases from about 0.05 mA/cm<sup>2</sup> at 0 rpm to 0.19 mA/cm<sup>2</sup> at 250 rpm. The highest current density is obtained at the electrode rotation rate of 500 rpm and decreases as the rotation rate increases. Based on this interpreted current density, the plating rate can be calculated and presented in Table 3. The highest plating rate is 0.76 μm/h (calculated by Faraday's law) obtained at the electrode

rotation rate of 500 rpm. The plating potential is slightly shifted to negative with increase in the electrode rotation rate from 0 to 500 rpm. Then, the shift to negative potential is quicker when the electrode rotation rate is > 500 rpm.

Fundamentally, a surface reaction of this electroless plating can be divided into the following steps[20]:

- Diffusion of reactants (2TMA-Au<sup>+</sup>, AET) to the surface;
- Adsorption of reactants at the surface;
- Chemical reaction on the surface;
- Desorption of by-products from the surface;
- Diffusion of by-products away from the surface.

The anodic current density increased with increase in the electrode rotation rate, indicating that the process of AET diffusion to the surface may determine the rate of the anodic reaction. In the cathodic region, the reaction was diffusion controlled at a rotation rate lower than 500 rpm. However, the reaction rate may depend on other

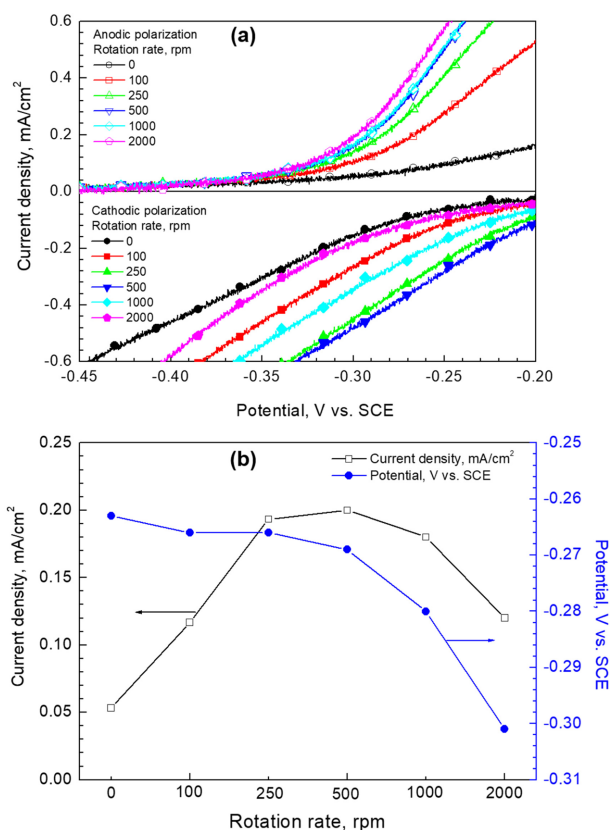


Fig. 3. Anodic and cathodic polarization curves of the basic electroless gold solution at different electrode rotation rates from 0 to 2000 rpm (a), mixed potential interpreted from polarization curves and current density at the mixed potential (b)

Table 3. Plating rate of the basic electroless gold solution calculated based on the interpreted current density at different electrode rotation rates

Electrode rotation rate, rpm	Plating rate, μm/h
0	0.203
100	0.444
250	0.736
500	0.762
1000	0.686
2000	0.457

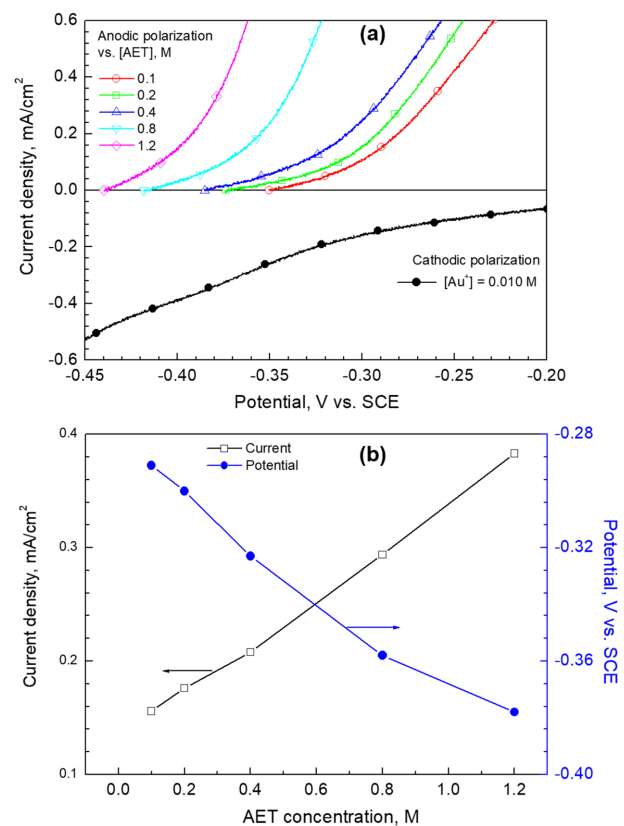


Fig. 4. Anodic polarization curve at different AET concentrations from 0.10 to 1.2 M (a), mixed potential interpreted from polarization curves and current density at the mixed potential (b), performed at 0.01 M Au<sup>+</sup>, 0.24 M TMA, pH 7.0 and temp. 80 °C

factors such as adsorption of the gold complex to the surface, the reaction at the surface, and the diffusion of by-products back into the solution.

Fig. 4a presents the anodic polarization curve at different AET concentrations from 0.10 to 1.2 M. The anodic curves shift to more negative potentials, and the slope of the current curves increase with increase in the AET concentration. This means that the reducing potential for Au<sup>+</sup> ions or the plating rate of an electroless gold bath increase with increase in the AET concentration. In fact, in general, in electroless plating solutions containing such as nickel and copper, the plating rate is always proportional to increase in the concentration of the reducing agent [20]. In this case, the role of the AET concentration in the electroless gold solution is similar. The mixed potential obtained from the polarization curves and current density at the mixed potential are shown in Fig. 4b. The interpreted current density was 0.16 mA/cm<sup>2</sup> at 0.10 M AET, linearly increases to 0.38 mA/cm<sup>2</sup> at 1.2 M AET, and the mixed potential shifts to more negative values. Although the rate of electroless plating increases with an increase in the reducing agent, it is limited by the stability of the bath and the quality of the coating.

Fig. 5 shows the cathodic polarization curves, mixed potential determined from polarization curves and current density at the mixed potential measured in the solution containing 0.40 M AET, 0.24 M TMA, and gold at different ion concentrations from 0.005 to 0.1 M. The significantly higher cathodic current density (0.21 mA/cm<sup>2</sup>) appears at the gold concentration of 0.01 M. In other cases, when the concentration of gold is lower or higher than 0.01 M, the current density at the mixed potential is always smaller. At Au<sup>+</sup> concentration of 0.025 M, the slope of the cathodic curve is significantly different from other concentrations. However, the reasons for this phenomenon are not clearly understood, and further studies are needed. The change in the mixed potential tends to be the same as the current density. According to this result, in the bath containing 0.40 M AET, the gold concentration of 0.01 M is the optimal concentration to achieve a sufficiently high plating rate in the electroless gold bath.

Fig. 6 presents the relationship between gold concentration, AET concentration, and current density at the mixed potential. When the AET concentration is less

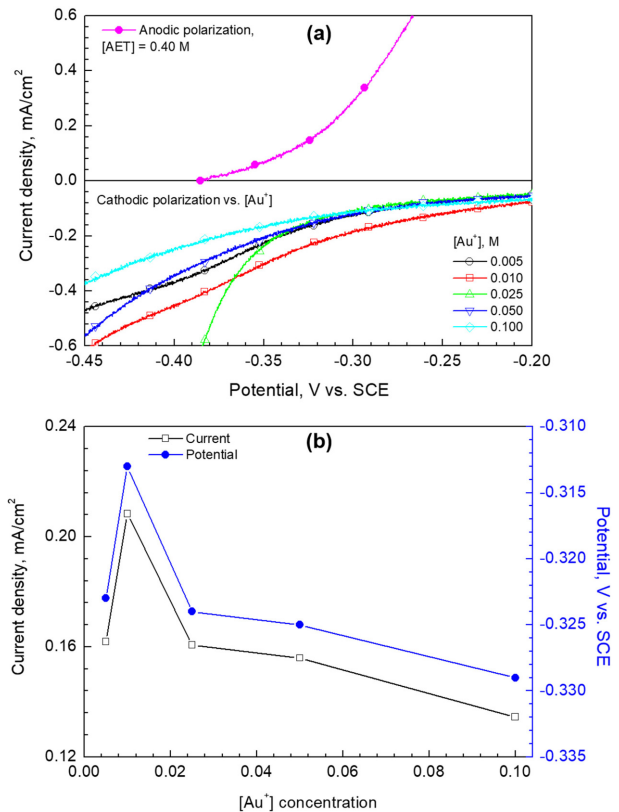


Fig. 5. Cathodic polarization curves at different Au<sup>+</sup> concentrations from 0.005 to 0.1 M (a), mixed potential interpreted from polarization curves and current density at the mixed potential (b), performed at 0.40 M AET, 0.24 M TMA, pH 7.0 and temp. 80 °C

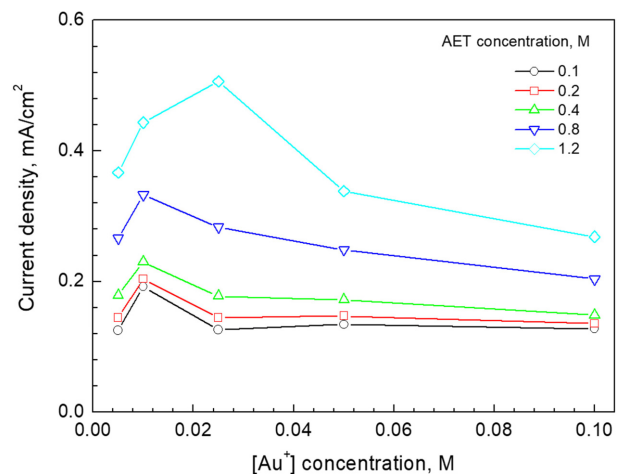


Fig. 6. Current density at the mixed potential interpreted from the polarization curve at different Au<sup>+</sup> and AET concentrations. Polarization curves performed at 0.24 M TMA, pH 7.0, temp. 80 °C and electrode rotation rate of 500 rpm

than 0.8 M, the dependence of the current density on the gold concentration is similar, with the highest current

intensity obtained at the gold concentration of 0.01 M. Only at the concentration of 1.2 M AET, the maximum current intensity occurred at the gold concentration of 0.025 M. This result again suggests that the optimal gold concentration to achieve the highest plating rate was about 0.01 M, regardless of the AET concentration. Because gold is costly, it is preferable to use it at low concentration while still achieving solution stability and plating rate. Therefore, the gold concentration of 0.01 M ( $\text{Au}^+ = 2.0 \text{ g/L}$ ) is suggested for this electroless gold plating bath with AET as the reducing agent.

Fig. 7a shows the effect of the TMA concentration on the cathodic polarization curves with the range of TMA concentrations from 0.08 to 0.40 M. It can be seen that the current density very rapidly decreases as the concentration of TMA increases. The mixed potential obtained from the polarization curves and current density at the mixed potential from  $[\text{AET}] = 0.40 \text{ M}$  are presented in Fig. 7b.

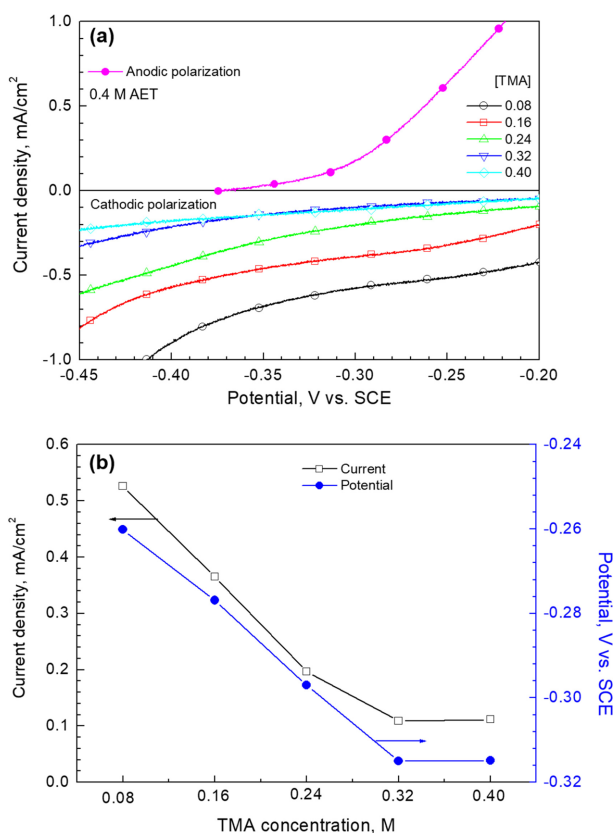
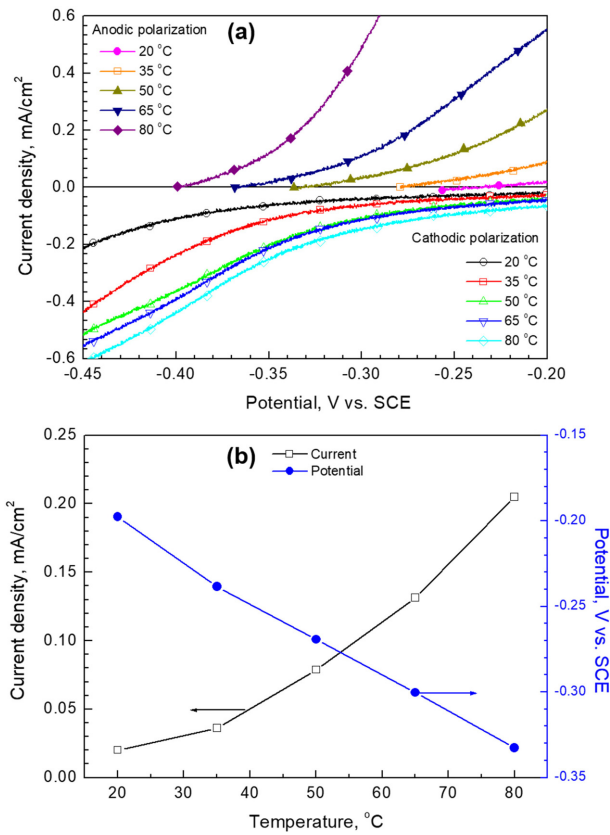


Fig. 7. Cathodic polarization curve at different TMA concentrations from 0.08 to 0.40 M (a), mixed potential interpreted from polarization curves and current density at the mixed potential (b), performed at 0.01 M  $\text{Au}^3$ , 0.40 M AET, pH 7.0 and temp. 80 °C

At 0.08 M TMA, the current density at the mixed potential is 0.53 mA/cm<sup>2</sup>, which rapidly decreases to 0.36 and 0.20 mA/cm<sup>2</sup> with the TMA concentrations of 0.16 and 0.24 M, respectively. After the TMA concentration reaches the critical value of 0.32 M, the increase in the TMA concentration no longer changes the current density. However, the current density is very low at that time: around 0.10 mA/cm<sup>2</sup>. The change in the potential with the TMA concentration is similar to the that of current density. As the TMA concentration increases, the mixed potential becomes more negative while the current density decreases. This means that the stability of the gold electroless plating bath will increase with increase in the TMA concentration.

In electroless plating solutions, organic acids are commonly used as complexing agents, particularly with an electroless nickel plating bath. The plating rate will increase as the complexing agent concentration reaches a critical value and then decreases as the complexing agent concentration increases. In this case, these organic acids are not only complexing agents but also buffers that act as accelerators, increasing the plating rate. For this gold electroless plating bath, gold ions can bond with TMA to form a 2TMA-Au complex, as discussed above. When the ratio  $[\text{TMA}] : [\text{Au}]$  is lower than 2, free gold ions will exist in the solution. Nevertheless, in the initial synthesis of the gold-TMA solution, the concentration  $[\text{TMA}] : [\text{Au}]$  ratio was 0.8:1.0, which is sufficient to keep the solution stable. In the gold electroless plating bath, because of the presence of the reducing agent, a higher concentration of complexing agent is required to ensure bath stability. The TMA concentration should be optimized to obtain a high plating rate while ensuring bath stability. In this work, high concentration of TMA was selected (0.24 M) for the electroless gold plating equivalent to  $[\text{TMA}] : [\text{Au}] = 24:1$ . In these conditions, the electrochemical plating solution has high stability and does not decompose after 24 h at 80 °C, even if a stabilizer is not used.

Fig. 8 presents the anodic and cathodic polarization curves of the basic gold electroless plating solution at different temperatures. The mixed potential obtained from the polarization curves and current density at the mixed potential. In general, the temperature is the most important parameter affecting the deposition rate of an electroless plating bath. The deposition rate is exponentially affected



**Fig. 8.** Anodic and cathodic polarization curves at different temperatures (a), mixed potential interpreted from polarization curves and current density at the mixed potential (b), performed at 0.01 M Au<sup>+</sup>, 0.40 M AET, 0.24 M TMA, and pH 7.0

by the temperature, and this relationship is independent of the acidity or alkalinity of the solution [34]. Fig. 8a shows that temperature has a significant influence on the anodic polarization curve. The anodic current density is close to zero at 20 °C, then rapidly increases with increasing temperature, in particular, from 65 to 80 °C. A similar result was obtained with the cathodic current density when increasing the bath temperature. However, the cathodic current density change is not very big compared to the that of anodic curve.

The current density at the mixed potential interpreted from polarization curves was about 0.008 mA/cm<sup>2</sup> at 20 °C, but increased to 0.08 and 0.20 mA/cm<sup>2</sup> at 50 and 80 °C, respectively. The mixed potential linearly decreased with increase in the temperature from 20 to 80 °C. These changes in current density and potential follow chemical thermodynamics and are similar to other electroless plating systems such as nickel and copper [20,35]. A

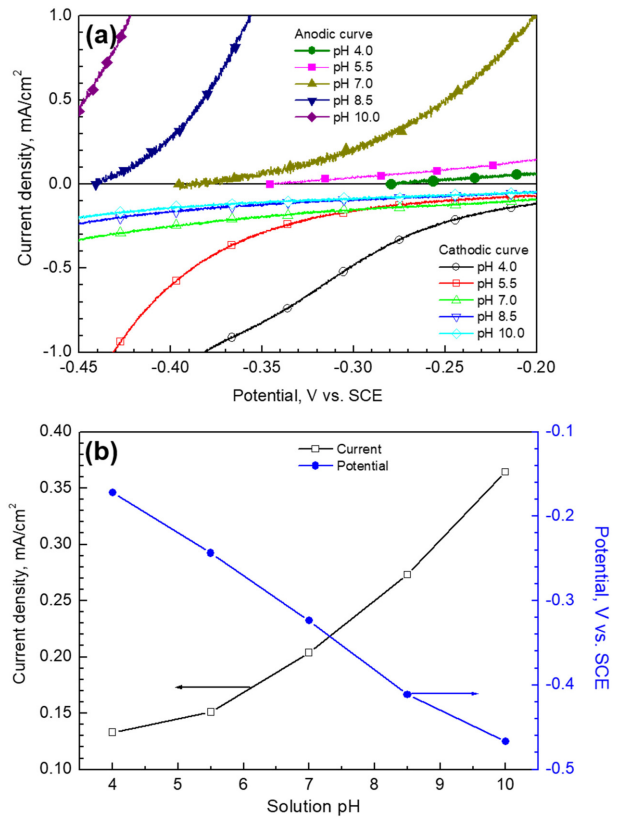


**Fig. 9.** Anodic and cathodic polarization curves at different solution pH (a), mixed potential interpreted from polarization curves and current density at the mixed potential (b), performed at 0.01 M Au<sup>+</sup>, 0.40 M AET, 0.24 M TMA, and temp. 80 °C

reaction at a higher temperature delivers more energy into the system and increases the reaction rate by causing more collisions between particles, as explained by collision theory [34]. Although the higher deposition rates make attractive results, there is danger due to the instability of the bath. Therefore, accurate temperature control is essential for electroless baths.

In addition to temperature, the anodic polarization curves are especially sensitive to the solution pH. Fig. 9 illustrates that the anodic current density dramatically increases with increase in the pH from 4 to 10. In an acidic medium (pH 4.0 and 5.5), the anode current density is close to zero. This means that the reducing power of AET increases in an alkaline medium. This property is similar to other reducing agents commonly used for electroless plating such as NaH<sub>2</sub>PO<sub>2</sub>, HCHO, NaBH<sub>4</sub>, and N<sub>2</sub>H<sub>2</sub> [20,35]. The cathode current density is low and slightly decreases as the pH increases from 7.0 to 10. It

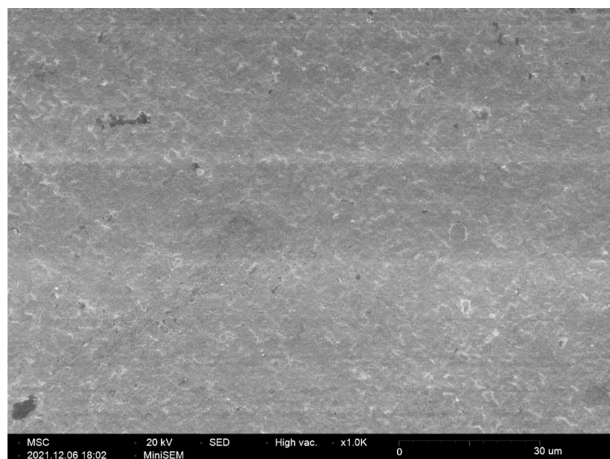


**Fig. 10.** SEM morphology of electroless gold plated on electroless nickel-phosphorus film, obtained from the basic electroless gold solution with a plating time of 30 min

is higher in the acidic medium. Although the trends in particular current densities of the anodic and cathodic parts are opposite to the change of pH, the current density (as calculated by the mixed potential theory) increases with increasing pH according to an exponential relationship. In contrast, the mixed potential becomes more negative in a linear relationship, as shown in Fig. 9b. Thus, the oxidation of AET can be explained using the following reaction [31]:



Fig. 10 displays the SEM morphology of the electroless gold obtained from the standard solution on electroless nickel-phosphorus film, with a plating time of 30 min. The standard solution contains 0.075 M  $\text{KH}_2\text{PO}_4$ , 0.24 M TMA, 0.01 M  $\text{Au}^+$ , and 0.40 M AET at pH 7.0 and 80 °C. On the surface, fine gold particles without any cracks can be observed. The coating thickness measured by X-ray fluorescence is 0.34  $\mu\text{m}$ , corresponding to a plating rate of about 0.68  $\mu\text{m}/\text{h}$ .

#### 4. Conclusions

In this work, a versatile non-cyanide electroless gold plating method using thiomalic acid (TMA) as a complexing agent and 2-aminoethanethiol (AET) as a reducing agent was developed. TMA can bond with  $\text{Au}^+$

to form high stable  $2\text{TMA-Au}^+$  complexes in solution. TMA is a potential candidate to replace the conventional toxic cyanide complex. AET can be a reducing agent for the electroless gold plating bath at a neutral pH. By measuring the partial anodic and cathodic polarization curves and using the mixed potential theory, it was determined that the highest current density was obtained at an electrode rotation rate from 250 to 500 rpm. The anodic polarization current density significantly increases with increase in the AET concentration, pH, and temperature. Increasing temperature also increases the cathodic current density; however, higher cathodic current density is obtained in a solution with lower pH. The current density of electroless plating or plating rate decreases with the increase in the TMA concentration. The cyanide free electroless gold solution containing 0.075 M  $\text{KH}_2\text{PO}_4$ , 0.24 M TMA, 0.01 M  $\text{Au}^+$ , and 0.40 M AET at pH 7.0 and 80 °C, has a plating rate of 0.68  $\mu\text{m}/\text{h}$  and high stability without stabilizers.

The TMA-base cyanide-free electroless gold plating solution newly developed by this study is expected to be applied to a wider range of industries because it is eco-friendly and can be used in a neutral pH range.

#### References

1. M. Kato and Y. Okinaka, Some recent developments in non-cyanide gold plating for electronics applications, *Gold Bulletin*, **37**, 37 (2004). Doi: <https://doi.org/10.1007/BF03215515>
2. R. J. Morrissey, A versatile non-cyanide gold plating system, *Plating and Surface Finishing*, **80**, 75 (1993). <https://www.nmfr.org/pdf/10493075.pdf>
3. Y. Okinaka and M. Hoshino, Some Recent Topics in Gold Plating for Electronics Applications, *Gold Bulletin*, **31**, 3 (1998). Doi: <http://dx.doi.org/10.1007/BF03215469>
4. T. Osaka, Y. Okinaka, J. Sasano, and M. Kato, Development of new electrolytic and electroless gold plating processes for electronics applications, *Science and Technology of Advanced Materials*, **7**, 425 (2006). Doi: <https://doi.org/10.1016/j.stam.2006.05.003>
5. H. O. Ali and I. R. Christie, A review of electroless gold deposition processes, *Gold Bulletin*, **17**, 118 (1984). Doi: <https://doi.org/10.1007/BF03214674>
6. M. Huang, X. Li, J. Xia, X. Li, W. Qiu, G. Zhang, R. Sun, and Y. Mu, *Proc. 2017 18th International Conference on*

- Electronic Packaging Technology (ICEPT) Conf.*, pp. 1173 - 1178, IEEE (2017).
7. H. Honma, Plating technology for electronics packaging, *Electrochimica Acta*, **47**, 75 (2001). Doi: [https://doi.org/10.1016/S0013-4686\(01\)00591-6](https://doi.org/10.1016/S0013-4686(01)00591-6)
  8. F. H. Reid, W. Goldie and E. W. Brooman, Gold Plating Technology, *Journal of The Electrochemical Society*, **122**, 188Ca (1975). Doi: <https://doi.org/10.1149/1.2134304>
  9. P. Wilkinson, Understanding gold plating, *Gold Bulletin*, **19**, 75 (1986). Doi: <https://doi.org/10.1007/BF03214646>
  10. Y. Okinaka, Electroless Gold Plating, *Journal of The Surface Finishing Society of Japan*, **42**, 1077 (1991). Doi: <https://doi.org/10.4139/sfj.42.1077>
  11. K. Wang, R. Beica, and N. Brown, *Proc. IEEE/CPMT/ SEMI 29th International Electronics Manufacturing Technology Symposium (IEEE Cat. No. 04CH37585)*, pp. 242 - 246, IEEE (2004).
  12. Y. Okinaka and M. Kato, Electroless deposition of gold, pp. 483 - 498, Wiley-VCH, Milan (2010).
  13. T. Green, M.-J. Liew, and S. Roy, Electrodeposition of Gold from a Thiosulfate-Sulfite Bath for Microelectronic Applications, *Journal of the electrochemical society*, **150**, C104 (2003). Doi: <https://doi.org/10.1149/1.1541006>
  14. T. Inoue, S. Ando, H. Okudaira, J. Ushio, A. Tomizawa, H. Takehara, T. Shimazaki, H. Yamamoto, and H. Yokono, *Proc. 45th Electronic Components and Technology Conf.*, pp. 1059 - 1067, IEEE (1995).
  15. Y. Sato, T. Osawa, K. Kaieda, and K. Kobayakawa, Cyanide-free electroless gold plating from a bath containing disulfiteaurate and thiourea or its derivatives, *Plating and surface finishing*, **81**, 74 (1994).
  16. T. Takeuchi, Y. Kohashi, D-H Kim, H. Nawafune, M. Tanikubo, and S. Mizumoto, Electroless Gold Plating Using L-cysteine as Reducing Agent & its Deposition Mechanism, *Plating and surface finishing*, **90**, 56 (2003).
  17. K. Vasilev, T. Zhu, G. Glasser, W. Knoll, and M. Kreiter, Preparation of Gold Nanoparticles in an Aqueous Medium Using 2-Mercaptosuccinic Acid as Both Reduction and Capping Agent, *Journal of nanoscience and nanotechnology*, **8**, 2062 (2008). Doi: <https://doi.org/10.1166/jnn.2008.057>
  18. A. M. Sullivan and P. A. Kohl, The autocatalytic deposition of gold in nonalkaline, gold thiosulfate electroless bath, *Journal of the Electrochemical Society*, **142**, 2250 (1995). Doi: <https://doi.org/10.1149/1.2044282>
  19. J. Hu, W. Li, J. Chen, X. Zhang, and X. Zhao, Novel plating solution for electroless deposition of gold film onto glass surface, *Surface and Coatings Technology*, **202**, 2922 (2008). Doi: <https://doi.org/10.1016/j.surfcoat.2007.10.026>
  20. G. O. Mallory and J. B. Hajdu, *Electroless plating: fundamentals and applications*, p. 401, William Andrew, Florida (1990).
  21. D. Baudrand and J. Bengston, Electroless plating processes, *Metal finishing*, **93**, 55 (1995). Doi: [https://doi.org/10.1016/0026-0576\(95\)99502-2](https://doi.org/10.1016/0026-0576(95)99502-2)
  22. C. G. Anderson, Alkaline sulfide gold leaching kinetics, *Minerals Engineering*, **92**, 248 (2016). Doi: <https://doi.org/10.1016/j.mineng.2016.01.009>
  23. T. Vorobyova, S. Poznyak, A. Rinskaya, and O. Vrublevskaya, Electroless gold plating from a hypophosphite-dicyanoaurate bath, *Surface and coatings technology*, **176**, 327 (2004). Doi: [https://doi.org/10.1016/S0257-8972\(03\)00744-8](https://doi.org/10.1016/S0257-8972(03)00744-8)
  24. M. I. Jeffrey and A. Angstetra, The Effect of Additives on the Electroless Deposition of Gold from a Thiosulfate-Ascorbic Acid Bath, *ECS Transactions*, **2**, 267 (2006). Doi: <https://doi.org/10.1149/1.2196016>
  25. M. Kato, K. Niikura, S. Hoshino, and I. Ohno, Electrochemical Behavior of Electroless Gold Plating with Ascorbic Acid as a Reducing Agent, *Journal of The Surface Finishing Society of Japan*, **42**, 729 (1991). Doi: <https://doi.org/10.4139/sfj.42.729>
  26. Y. Okinaka, An Electrochemical Study of Electroless Gold?Deposition Reaction, *Journal of the Electrochemical Society*, **120**, 739 (1973). Doi: <https://doi.org/10.1149/1.2403548>
  27. G. Corthey, L. J. Giovanetti, J. M. Ramallo-López, E. Zelaya, A. A. Rubert, G. A. Benitez, F. G. Requejo, M. H. Fonticelli, and R. C. Salvarezza, Synthesis and Characterization of Gold@Gold(I)-Thiomalate Core@Shell Nanoparticles, *ACS nano*, **4**, 3413 (2010). Doi: <https://doi.org/10.1021/nn100272q>
  28. D. J. LeBlanc, R. W. Smith, Z. Wang, H. E. Howard-Lock, and C. J. Lock, Thiomalate complexes of gold(I) : preparation, characterization and crystal structures of 1:2 gold to thiomalate complexes, *Journal of the Chemical Society, Dalton Transactions*, **18**, 3263 (1997). Doi: <https://doi.org/10.1039/A700827I>
  29. A. Bard, *Standard potentials in aqueous solution*, p. 313, Routledge, New York (2017). Doi: <https://doi.org/10.1201/9780203738764>
  30. H.K.Lee, D.H.Kim, D.K. Han, I.J.Son, Practical Surface Treatment Technology Series, *Electroless Plating*, **3**, 44

- (2014).
31. H. Nawafune, K. Shiroguchi, M. Tanikubo, S. Mizumoto, Y. Kohashi, and T. Takeuchi, Autocatalytic Electroless Silver Deposition Using 2-Aminoethanethiol as Reducing Agent, *Journal of The Surface Finishing Society of Japan*, **50**, 928 (1999). Doi: <https://doi.org/10.4139/sfj.50.928>
  32. I. Ohno, Electrochemistry of electroless plating, *Materials Science and Engineering : A*, **146**, 33 (1991). Doi: [https://doi.org/10.1016/0921-5093\(91\)90266-P](https://doi.org/10.1016/0921-5093(91)90266-P)
  33. A. J. Bard, G. Inzelt, and F. Scholz, *Electrochemical Dictionary*, p. 482, Springer Science & Business Media, Berlin (2008). Doi: <https://doi.org/10.1007/978-3-540-74598-3>
  34. M. L. Goldberger and K. M. Watson, *Collision theory*, p. 32, Courier Corporation, New York (2004).
  35. W. Riedel, Electroless nickel plating, ASM International (1991).